Divulgaciones Matemáticas Vol. 22, No. 1(2021), pp. 1–21

# Caputo and Caputo-Fabrizio fractional differential masks for images enhancement

*Máscaras diferenciales fraccionarias de Caputo y Caputo-Fabrizio para la mejora de imágenes*

Gustavo Asumu MBoro Nchama (asumu@matcom.uh.cu)
Universidad Nacional de Guinea Ecuatorial (UNGE)
Malabo, Guinea Ecuatorial, Calle Hassan II

Leandro Daniel Lau Alfonso (leandro@icimaf.cu)
Instituto de Cibernética Matemática y Física, ICIMAF
Calle 15, No. 551, entre C y D, Vedado, Habana 4, CP–10400, Cuba

Ana Luisa Morales Galloso (pedrosoaugusto584@gmail.com)
Facultad de Ciencias Medicas, Miguel Enríquez
Ramón Pinto y Ensenada Luyano, La Habana

**Abstract**

Image enhancement is one of the most important tasks in the field of image processing. With the help of computer and programming languages many mathematical methods have been implemented to improve the visual quality of an image. One of the most effective methods for this purpose is the histogram equalization. The construction of fractional differential masks for images enhancement has also been proposed. In this paper, we propose a new way of construction of fractional differential mask based on the Caputo and Caputo-Fabrizio derivatives. The effectiveness of the proposed methods have been compared with the histogram equalization method and the multiplication of each pixel of an image by a constant. The experiments results have shown superiority of the proposed methods, with better visual quality and higher gray-level co-occurrence matrix values in four directions.

**Key words and phrases:** Contrast image enhancement, fractional calculus, fractional differential mask.

**Resumen**

La mejora de imágenes es una de las tareas más importantes en el campo del procesamiento de imágenes. Con la ayuda de lenguajes informáticos y de programación, se han implementado muchos métodos matemáticos para mejorar la calidad visual de una imagen. Uno de los métodos más eficaces para este propósito es la ecualización del histograma. También se ha propuesto la construcción de máscaras diferenciales fraccionarias para la mejora de imágenes. En este artículo, se propone una nueva forma de construcción de máscara diferencial fraccional basada en las derivadas de Caputo y Caputo-Fabrizio. La eficacia de los métodos propuestos se ha comparado con el método de ecualización del histograma y la

Received 9/12/2020. Revised 12/01/2021. Accepted 11/04/2021.
MSC (2010): Primary 34Axx; Secondary 65Lxx.
Corresponding author: Gustavo Asumu MBoro Nchama

multiplicación de cada píxel de una imagen por una constante. Los resultados de los experimentos han demostrado la superioridad de los métodos propuestos, con una mejor calidad visual y valores de matriz de co-ocurrencia de nivel de gris más altos en cuatro direcciones.

**Palabras y frases clave:** Mejora de la imagen de contraste, cálculo fraccional, Máscara diferencial fraccionaria.

# 1 Introduction

Digital image processing is a set of techniques applied to digital images with the aim of improving their quality using a computer. For years, these type of techniques have been investigated and used in applications for different tasks such as image enhancement, image restoration and image edge detection, among others. For the image enhancement, various methods have been proposed: Histogram Equalization (HE) is one of the best used methods for image enhancement. It is provides better quality of images without loss of any information [12]. The multiplication of each pixel of an image by a constant is also one of the effective methods to make image clearer. Recently, many authors have proposed the construction of masks, for image enhancement, based on fractional derivatives [38-47]. A fractional derivative is an integral operator which generalizes the ordinary derivative, such that if the fractional derivative is represented by $D^\alpha$ then, when $\alpha = n$, it coincides with the usual differential operator $D^n$ [5]. Such kind of operators are defined by the help of spaces as:

**Definition 1.1.** A function $f : [a,b] \to \mathbb{R}$ is said to be absolutely continuous on $[a,b]$, denoted by $f \in AC[a,b]$, if given $\epsilon > 0$ there exists some $\sigma > 0$ such that

$$\sum_{k=1}^{n} |f(y_k) - f(x_k)| < \epsilon.$$

whenever $\{[x_k, y_k] : k = 1, \cdots, n\}$ is a finite collection of mutually disjoint subintervals of $[a,b]$ with

$$\sum_{k}^{n} (y_k - x_k) < \sigma.$$

**Definition 1.2.** Let $n \in \mathbb{N}$ and $k = 1, 2, \cdots, n-1$, the space $AC^n[a,b]$ is defined by

$$AC^n[a,b] := \{f : [a,b] \to \mathbb{R} : f^{(k)}(t) \in C[a,b], f^{(n-1)}(t) \in AC[a,b]\}.$$

There are many definitions of fractional derivatives [42-4]. One of the most popular was defined by Gronwald and Letnikov:

**Definition 1.3.** Let $a, b \in \mathbb{R}$ with $a < b$, $\alpha > 0$, $f \in C^n[a,b]$. The Gronwald-Letnikov $(GL)$ fractional derivative of order $\alpha$, is given by

$$^{GL}D^{\alpha}_{at} f(t) = \lim_{h \to 0^+} \frac{1}{h^\alpha} \sum_{k=0}^{\left[\frac{x-a}{h}\right]} (-1)^k \binom{\alpha}{k} f(t - kh). \tag{1}$$

where $\left[\frac{x-a}{h}\right]$ denotes the integer part of $\frac{x-a}{h}$.

One of the inconveniences of Gronwald-Letnikov derivative is that the class of functions for which this derivative is defined is very narrow. To overcome this inconvenience, Riemann and Liouville proposed the following definition [17]:

**Definition 1.4.** Let $a, b \in \mathbb{R}$ with $a < b$, $\alpha > 0$, $f \in AC^n[a,b]$. The Riemann-Liouville $(RL)$ fractional derivative of order $\alpha$, is defined by

$$ {}^{RL}D^{\alpha}_{at}f(t) = \frac{1}{\Gamma(n-\alpha)}\frac{d^n}{dt^n}\int_a^t (t-s)^{n-(\alpha+1)}f(s)ds. $$

Even though the $RL$ approach overcomes the drawbacks related the $GL$ definition and it has been applied successfully in many areas of engineering, unfortunately, it leads to initial conditions containing the limit values of the $RL$ fractional derivative at the lower terminal $t = a$, for example

$$ \lim_{t\to a}\{{}^{RL}D^{\alpha-1}_{at}f(t)\} = b_1, \quad \lim_{t\to a}\{{}^{RL}D^{\alpha-2}_{at}f(t)\} = b_2, \quad \ldots, \quad \lim_{t\to a}\{{}^{RL}D^{\alpha-n}_{at}f(t)\} = b_n. $$

In spite of the fact that initial value problems with such initial conditions can be successfully solved mathematically, their solutions are practically useless, because there is no known physical interpretation for such types of initial conditions. An alternative solution to this conflict was proposed by M. Caputo [17]:

**Definition 1.5.** Let $a, b \in \mathbb{R}$ with $a < b$, $\alpha > 0$, $f \in AC^n[a,b]$. The Caputo fractional derivative of order $\alpha$, is defined by

$$ {}^{C}D^{\alpha}_{at}f(t) = \frac{1}{\Gamma(n-\alpha)}\int_a^t (t-s)^{n-(\alpha+1)}f^{(n)}(s)ds. \tag{2} $$

For $0 < \alpha \leq 1$ and $a = 0$, the numerical approximation of (2) takes the form

$$ {}^{C}D^{\alpha}_{0x}u(x) = \frac{1}{\Gamma(1-\alpha)}\int_0^x (x-\xi)^{-\alpha}u'(\xi)d\xi \approx \frac{1}{\Gamma(1-\alpha)}\sum_{k=0}^{N-1}\int_{\frac{kx}{N}}^{\frac{(k+1)x}{N}} (x-\xi)^{-\alpha}u'(\xi_k)d\xi. \tag{3} $$

To describe material heterogeneity and structures with different scales which cannot be well described by classical local theories or by fractional models with singular kernel, Caputo and Fabrizio introduced a new fractional approach [7]:

**Definition 1.6.** Let $a, b \in \mathbb{R}$ with $a < b$, $0 < \alpha < 1$, $f \in AC^1[a,b]$. The Caputo-Fabrizio fractional derivative of order $\alpha$, is defined by

$$ {}^{CF}D^{\alpha}_{ax}u(x) = \frac{M(\alpha)}{1-\alpha}\int_a^x e^{-\frac{\alpha}{1-\alpha}(x-s)}u'(s)ds, $$

where $M(\alpha)$ is a function such that $M(0) = M(1) = 1$.

In [24], Losada and Nieto, suggested the following particular case

$$ \begin{aligned} {}^{CF}D^{\alpha}_{ax}u(x) &= \frac{1}{1-\alpha}\int_a^x e^{-\frac{\alpha}{1-\alpha}(x-s)}u'(s)ds \\ &= \frac{1}{1-\alpha}\Big(u(x) - e^{-\frac{\alpha}{1-\alpha}x}u(a)\Big) - \frac{\alpha}{(1-\alpha)^2}\int_a^x e^{-\frac{\alpha}{1-\alpha}(x-\tau)}u(\tau)d\tau. \end{aligned} \tag{4} $$

Taking $a = 0$, formula (4) can be approximated as

$$ {}^{CF}D_{0x}^{\alpha}u(x) = \frac{1}{1-\alpha}\int_0^x e^{-\frac{\alpha}{1-\alpha}(x-\xi)}u'(\xi)d\xi \approx \frac{1}{1-\alpha}\sum_{k=0}^{N-1}\int_{\frac{kx}{N}}^{\frac{(k+1)x}{N}} e^{-\frac{\alpha}{1-\alpha}(x-\xi)}u'(\xi_k)d\xi. \quad (5) $$

Fractional derivatives provide interesting possibilities for scientific fields such as anomalous diffusion [40-23], circuit theory [3-43], image processing [33-26] and many others [1-29]. The purpose of this paper is to improve the visual quality of dark images by using Fractional Differential Masks in Caputo (FDMC) and Caputo-Fabrizio (FDMCF) senses. The remainder of this paper is organized as follows: in section 2, we construct a fractional differential mask in the Caputo sense, next, fractional differential mask in Caputo-Fabrizio sense is given in section 3. Section 4 presents the experimental results of the proposed methods. A conclusion is considered in section 5.

## 2 Prewitt fractional filter in the Caputo sense

The goal of this section is to costruct a fractional differential mask based on the Caputo derivative definition. For this purpose, we first discretize numerically the Caputo derivative based on the forward finite difference scheme in the interval $[0, x]$ (analogously $[0, y]$). Let's take a partition of $N$ nodes of the interval $[0, x]$, with step $\Delta x = \dfrac{x}{N}$. Thus, there are $N + 1$ nodes. The $N + 1$ causal pixels can be given by

$$ \begin{cases} u_0 = u(0) \\ u_1 = u(\frac{x}{N}) \\ \vdots \\ u_k = u(\frac{kx}{N}) \\ \vdots \\ u_N = u(x), \end{cases} $$

For $\alpha \in (0, 1)$, by approximating, we obtain

$$ \begin{aligned} \int_{\frac{kx}{N}}^{\frac{(k+1)x}{N}} (x-\xi)^{-\alpha}u'(\xi_k)d\xi \;&\approx\; \frac{u\left(\frac{kx+x}{N}\right) - u\left(\frac{kx}{N}\right)}{\Delta x}\int_{\frac{kx}{N}}^{\frac{kx+x}{N}} (x-\xi)^{-\alpha}d\xi \\ &=\; \frac{u\left(\frac{kx+x}{N}\right) - u\left(\frac{kx}{N}\right)}{-(1-\alpha)(\Delta x)^{\alpha}}\left[(N-k-1)^{1-\alpha} - (N-k)^{1-\alpha}\right]. \end{aligned} \quad (6) $$

Then, taking (6) into (3), we have

$$
\begin{aligned}
{}^{C}D_{0x}^{\alpha}u(x) &\approx \frac{1}{(\Delta x)^{\alpha}\Gamma(2-\alpha)}\sum_{k=0}^{N-1}\left\{\left[u\left(\frac{(k+1)x}{N}\right)-u\left(\frac{kx}{N}\right)\right]\left[(N-k-1)^{1-\alpha}-(N-k)^{1-\alpha}\right]\right\} \\
&= \frac{1}{(\Delta x)^{\alpha}\Gamma(2-\alpha)}\left\{\begin{array}{c}
1^{1-\alpha}u_N+\left(2^{1-\alpha}-2\cdot 1^{1-\alpha}\right)u_{N-1} \\
+\left(2\cdot 2^{1-\alpha}-3^{1-\alpha}-1^{1-\alpha}\right)u_{N-2} \\
+\left[(N-j-1)^{1-\alpha}+(N-j+1)^{1-\alpha}\right. \\
\left.-2(N-j)^{1-\alpha}\right]u_j+\cdots+\left[(N-2)^{1-\alpha}\right. \\
\left.-2(N-1)^{1-\alpha}+N^{1-\alpha}\right]u_1 \\
+\left[(N-1)^{1-\alpha}-N^{1-\alpha}\right]u_0
\end{array}\right\}. \qquad (7)
\end{aligned}
$$

The anterior approximate difference of fractional partial differential on $x$ and $y$ coordinates are expressed as

$$
{}^{C}D_{0x}^{\alpha}u(x,y) \approx \frac{1}{(\Delta x)^{\alpha}\Gamma(2-\alpha)}\left\{\begin{array}{c}
1^{1-\alpha}u(x,y)+\left(2^{1-\alpha}-2\cdot 1^{1-\alpha}\right)u(x-1,y) \\
+\left(2\cdot 2^{1-\alpha}-3^{1-\alpha}-1^{1-\alpha}\right)u(x-2,y) \\
+\cdots+\left[(N-1)^{1-\alpha}-N^{1-\alpha}\right]u(x-n,y)
\end{array}\right\}, \qquad (8)
$$

and

$$
{}^{C}D_{0y}^{\alpha}u(x,y) \approx \frac{1}{(\Delta x)^{\alpha}\Gamma(2-\alpha)}\left\{\begin{array}{c}
1^{1-\alpha}u(x,y)+\left(2^{1-\alpha}-2\cdot 1^{1-\alpha}\right)u(x,y-1) \\
+\left(2\cdot 2^{1-\alpha}-3^{1-\alpha}-1^{1-\alpha}\right)u(x,y-2) \\
+\cdots+\left[(N-1)^{1-\alpha}-N^{1-\alpha}\right]u(x,y-n)
\end{array}\right\}. \qquad (9)
$$

As in a digital 2-$D$ gray image $u(x,y)$, the shortest distance on $x$ and $y$ coordinates is one pixel, then we put $\Delta x = \Delta y = 1$, and from (7), we obtain $N+1$ coefficients $c_i$ $(i = 0,\ldots,N)$, which depend on the fractional order $\alpha$:

$$\begin{cases} c_0 = \dfrac{1^{1-\alpha}}{\Gamma(2-\alpha)}, \\ c_1 = \dfrac{2^{1-\alpha} - 2 \cdot 1^{1-\alpha}}{\Gamma(2-\alpha)}, \\ c_2 = \dfrac{2 \cdot 2^{1-\alpha} - 3^{1-\alpha} - 1^{1-\alpha}}{\Gamma(2-\alpha)}, \\ \vdots \\ c_j = \dfrac{(N-j-1)^{1-\alpha} + (N-j+1)^{1-\alpha} - 2(N-j)^{1-\alpha}}{\Gamma(2-\alpha)}, \\ \vdots \\ c_N = \dfrac{(N-1)^{1-\alpha} - N^{1-\alpha}}{\Gamma(2-\alpha)}. \end{cases}$$

## 3 Prewitt fractional filter in the Caputo-Fabrizio sense

Following the idea as in the previous section, we obtain

$$\begin{aligned} \int_{\frac{kx}{N}}^{\frac{(k+1)x}{N}} e^{-\frac{\alpha}{1-\alpha}(x-\xi)} u'(\xi_k) d\xi &\approx \frac{u\left(\frac{kx+x}{N}\right) - u\left(\frac{kx}{N}\right)}{\Delta x} \int_{\frac{kx}{N}}^{\frac{kx+x}{N}} e^{-\frac{\alpha}{1-\alpha}(x-\xi)} d\xi, \\ &= \frac{1-\alpha}{\alpha} \cdot \frac{u\left(\frac{kx+x}{N}\right) - u\left(\frac{kx}{N}\right)}{\Delta x} \cdot \left[e^{-\frac{\alpha(N-k-1)\Delta x}{1-\alpha}} - e^{-\frac{\alpha(N-k)\Delta x}{1-\alpha}}\right]. \end{aligned} \tag{10}$$

Inserting (10) into (5), we have

$$\begin{aligned} {}^{CF}D_{0x}^{\alpha} u(x) &\approx \frac{1}{\alpha} \sum_{k=0}^{N-1} \left\{ \left[ \frac{u\left(\frac{(k+1)x}{N}\right) - u\left(\frac{kx}{N}\right)}{\frac{x}{N}} \right] \left[ e^{-\frac{\alpha}{1-\alpha}[N-(k+1)]\frac{x}{N}} - e^{-\frac{\alpha}{1-\alpha}[N-k]\frac{x}{N}} \right] \right\} \\ &= \frac{1}{\alpha \cdot \Delta x} \left\{ \begin{array}{c} \left(1 - e^{-\frac{\alpha}{1-\alpha}\Delta x}\right) u_N + \left(2e^{-\frac{\alpha \cdot \Delta x}{1-\alpha}} - e^{-2\frac{\alpha \cdot \Delta x}{1-\alpha}} - 1\right) u_{N-1} + \\ \left(2e^{-\frac{2\alpha \cdot \Delta x}{1-\alpha}} - e^{-3\frac{\alpha \cdot \Delta x}{1-\alpha}} - e^{-\frac{\alpha \cdot \Delta x}{1-\alpha}}\right) u_{N-2} + \cdots + \\ \left(2e^{-\frac{\alpha \cdot (N-j) \cdot \Delta x}{1-\alpha}} - e^{-\frac{\alpha \cdot (N-j-1) \cdot \Delta x}{1-\alpha}} - e^{-\frac{\alpha \cdot (N-j+1) \cdot \Delta x}{1-\alpha}}\right) u_j \\ + \cdots + \left(2e^{-\frac{\alpha \cdot (N-1) \cdot \Delta x}{1-\alpha}} - e^{-\frac{\alpha \cdot (N-2) \cdot \Delta x}{1-\alpha}} - e^{-\frac{\alpha \cdot N \cdot \Delta x}{1-\alpha}}\right) u_1 \\ + \left(2e^{-\frac{\alpha \cdot N \cdot \Delta x}{1-\alpha}} - e^{-\frac{\alpha \cdot (N-1) \cdot \Delta x}{1-\alpha}} - e^{-\frac{\alpha \cdot (N+1) \cdot \Delta x}{1-\alpha}}\right) u_0 \end{array} \right\}. \end{aligned} \tag{11}$$

From (11), we obtain $N+1$ nonzero coefficients $c_i$ $(i=0,\dots,N)$, given by

$$\begin{cases} c_0 = \dfrac{1}{\alpha\Delta x}\left(1 - e^{-\frac{\alpha}{1-\alpha}\Delta x}\right), \\ c_1 = \dfrac{1}{\alpha\Delta x}\left(2e^{-\frac{\alpha}{1-\alpha}\Delta x} - e^{-\frac{2\alpha}{1-\alpha}\Delta x} - 1\right), \\ c_2 = \dfrac{1}{\alpha\Delta x}\left(2e^{-2\frac{\alpha}{1-\alpha}\Delta x} - e^{-3\frac{\alpha}{1-\alpha}\Delta x} - e^{-\frac{\alpha}{1-\alpha}\Delta x}\right), \\ \vdots \\ c_j = \dfrac{1}{\alpha\Delta x}\left(2e^{-\frac{\alpha}{1-\alpha}(N-j)\Delta x} - e^{-\frac{\alpha}{1-\alpha}(N-j-1)\Delta x} - e^{-\frac{\alpha}{1-\alpha}(N-j+1)\Delta x}\right), \\ \vdots \\ c_{N-1} = \dfrac{1}{\alpha\Delta x}\left(2e^{-\frac{\alpha}{1-\alpha}(N-1)\Delta x} - e^{-\frac{\alpha}{1-\alpha}(N-2)\Delta x} - e^{-\frac{\alpha}{1-\alpha}N\Delta x}\right), \\ c_N = \dfrac{1}{\alpha\Delta x}\left(2e^{-\frac{\alpha}{1-\alpha}N\Delta x} - e^{-\frac{\alpha}{1-\alpha}(N-1)\Delta x} - e^{-\frac{\alpha}{1-\alpha}(N+1)\Delta x}\right). \end{cases}$$

Taking $\Delta x = \Delta y = 1$, as in the previous section, we obtain the followings two expressions:

$${}^{CF}D^{\alpha}_{0y}u(x,y) \approx \frac{1}{\alpha}\left\{ \begin{array}{c} \left(1 - e^{-\frac{\alpha}{1-\alpha}}\right)u(x,y) + \left(2e^{-\frac{\alpha}{1-\alpha}} - e^{-2\frac{\alpha}{1-\alpha}} - 1\right)u(x-1,y) \\ +\left(2e^{-2\frac{\alpha}{1-\alpha}} - e^{-3\frac{\alpha}{1-\alpha}} - e^{-\frac{\alpha}{1-\alpha}}\right)u(x-2,y) + \cdots \\ +\left(2e^{-\frac{\alpha}{1-\alpha}N} - e^{-\frac{\alpha}{1-\alpha}(N-1)} - e^{-\frac{\alpha}{1-\alpha}(N+1)}\right)u(x-n,y) \end{array} \right\}, \tag{12}$$

and

$${}^{CF}D^{\alpha}_{0y}u(x,y) \approx \frac{1}{\alpha}\left\{ \begin{array}{c} \left(1 - e^{-\frac{\alpha}{1-\alpha}}\right)u(x,y) + \left(2e^{-\frac{\alpha}{1-\alpha}} - e^{-2\frac{\alpha}{1-\alpha}} - 1\right)u(x,y-1) \\ +\left(2e^{-2\frac{\alpha}{1-\alpha}} - e^{-3\frac{\alpha}{1-\alpha}} - e^{-\frac{\alpha}{1-\alpha}}\right)u(x,y-2) + \cdots \\ +\left(2e^{-\frac{\alpha}{1-\alpha}N} - e^{-\frac{\alpha}{1-\alpha}(N-1)} - e^{-\frac{\alpha}{1-\alpha}(N+1)}\right)u(x,y-n) \end{array} \right\}. \tag{13}$$

The next images show the results of applying the proposed FDMCF, with different values of differential order $\alpha$, on the following images: goldhill image, drak bedroom and dark room.

(a) Original image

(b) $\alpha = 0.0071$

(c) $\alpha = 0.0072$

(d) $\alpha = 0.0073$

(e) $\alpha = 0.0074$

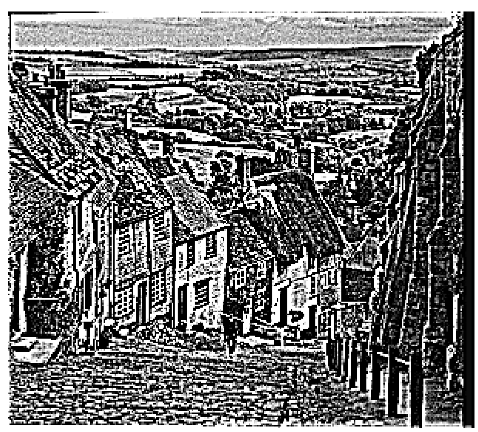

(f) $\alpha = 0.0075$

Figure 1: Result of applying the proposed FDMCF on goldhill image with different values of differential order $\alpha$.

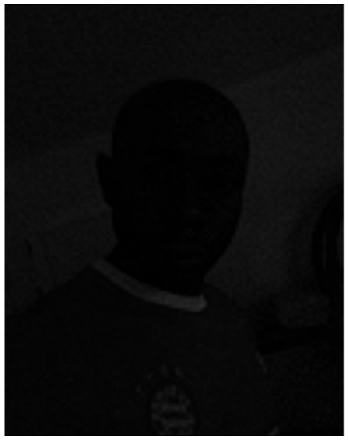

(a) Original image

(b) $\alpha = 0.003$

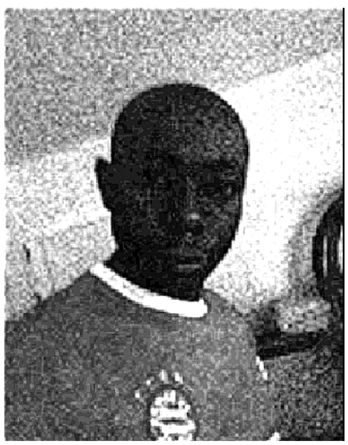

(c) $\alpha = 0.004$

(d) $\alpha = 0.005$

(e) $\alpha = 0.006$

(f) $\alpha = 0.007$

Figure 2: Result of applying the proposed FDMCF on a dark bedroom image with different values of differential order $\alpha$.

(a) Original image

(b) $\alpha = 0.003$

(c) $\alpha = 0.004$

(d) $\alpha = 0.005$

(e) $\alpha = 0.006$

(f) $\alpha = 0.007$

Figure 3: Result of applying the proposed FDMCF on a dark room image with different values of differential order $\alpha$.

The next tables show the results of contrast in terms of the Gray-Level Co-occurrence Matrix (GLCM) in 4 directions, on the following images: goldhill image, drak bedroom and dark room.

| | | Angle | | | |
|---|---|---|---|---|---|
| | | $0^0$ | $45^0$ | $90^0$ | $135^0$ |
| Original image | | 0.2743 | 0.5685 | 0.4336 | 0.5542 |
| Method | HE | 0.5018 | 0.9403 | 0.6727 | 0.9352 |
| | MPIT | 0.4642 | 0.8428 | 0.6060 | 0.8476 |
| | FDMC for $\alpha = 0.0155$ | 7.4922 | 11.7211 | 8.8573 | 11.5499 |
| | FDMC for $\alpha = 0.0165$ | 13.0910 | 18.5857 | 12.7200 | 18.6007 |
| | FDMC for $\alpha = 0.0170$ | 15.1278 | 20.5889 | 13.4156 | 20.7000 |
| | FDMCF for $\alpha = 0.0071$ | 9.0089 | 12.3465 | 8.7710 | 12.4288 |
| | FDMCF for $\alpha = 0.0072$ | 9.5492 | 12.8873 | 9.0874 | 13.0488 |
| | FDMCF for $\alpha = 0.0073$ | 9.9501 | 13.2338 | 9.2318 | 13.4732 |

Table 1: Gold-hill image.

| | | Angle | | | |
|---|---|---|---|---|---|
| | | $0^0$ | $45^0$ | $90^0$ | $135^0$ |
| Original image | | 0.0007 | 0.0888 | 0.0885 | 0.0888 |
| Method | HE | 0.2229 | 0.3526 | 0.2241 | 0.3632 |
| | MPITH | 0.1345 | 0.2625 | 0.1488 | 0.2638 |
| | FDMC for $\alpha = 0.013$ | 0.7667 | 1.4983 | 1.0776 | 1.5015 |
| | FDMC for $\alpha = 0.014$ | 0.7653 | 1.4477 | 1.0253 | 1.4494 |
| | FDMC for $\alpha = 0.015$ | 0.7172 | 1.4236 | 1.0371 | 1.4240 |
| | FDMCF for $\alpha = 0.005$ | 0.6574 | 1.0510 | 0.6768 | 1.0653 |
| | FDMCF for $\alpha = 0.006$ | 0.6459 | 0.9865 | 0.6296 | 0.9923 |
| | FDMCF for $\alpha = 0.007$ | 0.5014 | 0.7176 | 0.4438 | 0.7180 |

Table 2: Dark bedroom.

| | | Angle | | | |
|---|---|---|---|---|---|
| | | $0^0$ | $45^0$ | $90^0$ | $135^0$ |
| Original image | | 0.4711 | 0.6691 | 0.2139 | 0.6694 |
| Method | HE | 0.6178 | 0.8568 | 0.5153 | 0.8977 |
| | MPITH | 0.4221 | 0.7419 | 0.4225 | 0.7560 |
| | FDMC for $\alpha = 0.013$ | 3.5218 | 5.4161 | 3.4127 | 5.4255 |
| | FDMC for $\alpha = 0.014$ | 3.6872 | 5.8437 | 3.7464 | 5.8422 |
| | FDMC for $\alpha = 0.015$ | 3.8128 | 6.0092 | 3.8800 | 6.0260 |
| | FDMCF for $\alpha = 0.005$ | 2.4504 | 3.9630 | 2.6457 | 3.9593 |
| | FDMCF for $\alpha = 0.006$ | 2.5697 | 4.2178 | 2.8633 | 4.1469 |
| | FDMCF for $\alpha = 0.007$ | 2.7114 | 4.0842 | 2.6762 | 4.0415 |

Table 3: Dark room.

The following images show the comparison of contrast enhancement capability between the methods: MPIT; MPITH; HE; FDMC; and FDMCF applied to the *Goldhill image*.

(a) Original image

(b) MPIT

(c) MPITH

(d) HE

(e) FDMC with $\alpha = 0.0155$

(f) FDMCF with $\alpha = 0.0072$

Figure 4: Comparison of contrast enhancement capability between methods.

The next images show the comparison of contrast enhancement capability between the methods: MPIT; MPITH; HE; FDMC; and FDMCF applied to the *Dark Bedroom image*.

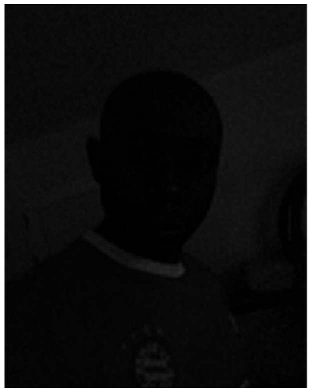

(a) Original image

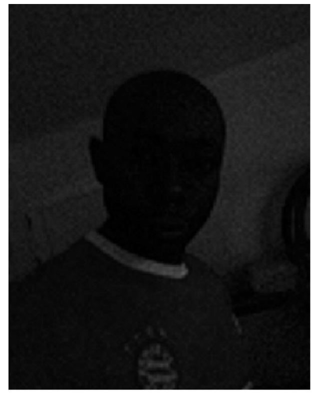

(b) MPIT

(c) MPITH

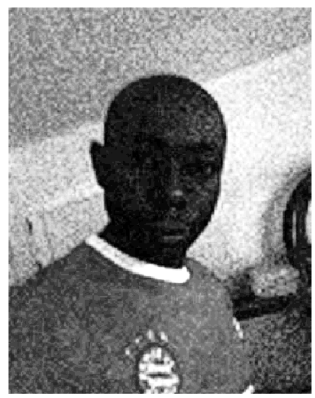

(d) HE

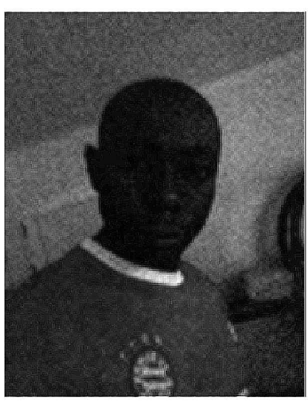

(e) FDMC with $\alpha = 0.014$

(f) FDMCF with $\alpha = 0.006$

Figure 5: Comparison of contrast enhancement capability between methods.

The next images show the comparison of contrast enhancement capability between the methods: MPIT; MPITH; HE; FDMC; and FDMCF applied to the *Dark room image*.

(a) Original image

(b) MPIT

(c) MPITH

(d) HE

(e) FDMC with $\alpha = 0.013$

(f) FDMCF with $\alpha = 0.005$

Figure 6: Comparison of contrast enhancement capability between methods.

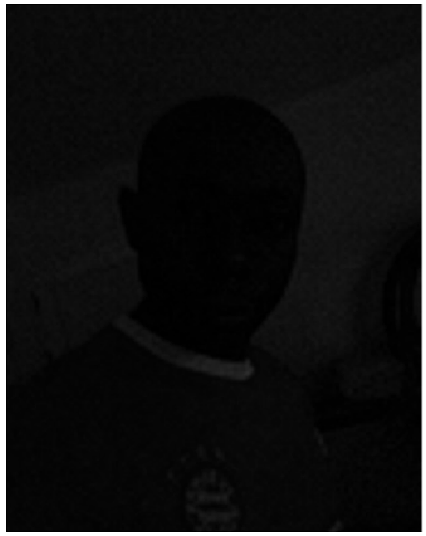

(a) Dark bedroom image

(b) Dark room image

(c) Gold-hill image

Figure 7: Original images used in the experimental result.

# 4 Experimental results

The aim of this section is to demonstrate that fractional differential masks based on Caputo (FDMC) and Caputo-Fabrizio (FDMCF) definitions have better capability in texture-enhancing than the traditional approaches for texture-rich image. To this purpose, we analyze the texture-enhancing capability of the proposed masks and discuss the relationship between fractional power parameter $\alpha$ and texture-enhancing details by using Gray-Level Co-occurrence Matrix (GLCM). Finally, we discuss the capability of texture enhancement of the proposed masks by making comparison with Histogram Equalization (HE), Multiplication of each Pixel of an Image by Two (MPIT) and Multiplication of each Pixel of an Image by Three (MPITH) methods. Three images used in the experimental results are shown in Figures 7. First is dark bedroom image, second is a dark room image, the third one is the gold-hill image. To obtain the fractional differential on the eight symmetric directions and make the fractional differential masks have anti-rotation capability, eight fractional differential masks which are respectively on the directions of $0^0$, $45^0$, $90^0$, $135^0$, $180^0$, $225^0$, $270^0$ and $315^0$ are implemented in Fig. 8. Considering

$$sum = \frac{c_0 + c_1 + c_2 + \cdots + c_n}{8}$$

and taking into account the eight neighboring pixels of a given one, we propose the fractional differential mask, given by Table 4.

| | | | | | | |
|---|---|---|---|---|---|---|
| $C_n$ | 0 | 0 | $C_n$ | 0 | 0 | $C_n$ |
| 0 | $\ddots$ | 0 | $\vdots$ | 0 | $\ddots$ | 0 |
| $\vdots$ | 0 | $C_1$ | $C_1$ | $C_1$ | 0 | $\vdots$ |
| $C_n$ | $\cdots$ | $C_1$ | $sum$ | $C_1$ | $\cdots$ | $C_n$ |
| $\vdots$ | 0 | $C_1$ | $C_1$ | $C_1$ | 0 | $\vdots$ |
| 0 | $\ddots$ | 0 | $\vdots$ | 0 | $\ddots$ | 0 |
| $C_n$ | 0 | 0 | $C_n$ | 0 | 0 | $C_n$ |

Table 4: Fractional differential mask.

For the implementation of the FDMCF method, we have taken only the following three coefficients:

$$\begin{aligned} c_0 &= \frac{1}{\alpha}\left(1 - e^{-\frac{\alpha}{1-\alpha}}\right), \\ c_1 &= \frac{1}{\alpha}\left(2e^{-\frac{\alpha}{1-\alpha}} - e^{-\frac{2\alpha}{1-\alpha}} - 1\right), \\ c_2 &= \frac{1}{\alpha}\left(2e^{-2\frac{\alpha}{1-\alpha}} - e^{-3\frac{\alpha}{1-\alpha}} - e^{-\frac{\alpha}{1-\alpha}}\right), \end{aligned}$$

while for the FDMC method, we considered the coefficients:

$$c_0 = \frac{1^{1-\alpha}}{\Gamma(2-\alpha)}, \qquad c_1 = \frac{2^{1-\alpha} - 2 \cdot 1^{1-\alpha}}{\Gamma(2-\alpha)}, \qquad c_2 = \frac{2 \cdot 2^{1-\alpha} - 3^{1-\alpha} - 1^{1-\alpha}}{\Gamma(2-\alpha)},$$

| | | | | | | | | |
|---|---|---|---|---|---|---|---|---|
| $c_0$ | 0 | … | | | | | | |
| 0 | $c_1$ | 0 | … | | | | | |
| ⋮ | 0 | $c_2$ | 0 | | | | | |
| | ⋮ | 0 | ⋱ | ⋱ | | | | |
| | | ⋮ | 0 | $c_k$ | 0 | ⋮ | | |
| | | | ⋮ | ⋱ | ⋱ | 0 | … | |
| | | | | … | 0 | $c_{N-2}$ | 0 | ⋮ |
| | | | | | … | 0 | $c_{N-1}$ | 0 |
| | | | | | | … | 0 | $c_N$ |

Mask in the direction of $315^0$

| | | | | | | | | |
|---|---|---|---|---|---|---|---|---|
| | | | | | | … | 0 | $c_N$ |
| | | | | | … | 0 | $c_{N-1}$ | 0 |
| | | | | … | 0 | $c_{N-2}$ | 0 | ⋮ |
| | | | | ⋱ | ⋱ | 0 | ⋮ | |
| | | … | 0 | $c_k$ | 0 | … | | |
| | ⋮ | 0 | ⋱ | ⋱ | ⋱ | | | |
| ⋮ | 0 | $c_2$ | 0 | … | | | | |
| 0 | $c_1$ | 0 | … | | | | | |
| $c_0$ | 0 | … | | | | | | |

Mask in the direction of $45^0$

| | | | | | | | | |
|---|---|---|---|---|---|---|---|---|
| | | … | 0 | $c_N$ | 0 | … | | |
| | | … | 0 | $c_{N-1}$ | 0 | … | | |
| | | … | 0 | $c_{N-2}$ | 0 | … | | |
| | | | ⋮ | ⋮ | ⋮ | | | |
| | | … | 0 | $c_k$ | 0 | … | | |
| | | | ⋮ | ⋮ | ⋮ | | | |
| | | … | 0 | $c_2$ | 0 | … | | |
| | | … | 0 | $c_1$ | 0 | … | | |
| | | … | 0 | $c_0$ | 0 | … | | |

Mask in the direction of $90^0$

| | | | | | | | | |
|---|---|---|---|---|---|---|---|---|
| | | … | 0 | $c_0$ | 0 | … | | |
| | | … | 0 | $c_1$ | 0 | … | | |
| | | … | 0 | $c_2$ | 0 | … | | |
| | | | ⋮ | ⋮ | ⋮ | | | |
| | | … | 0 | $c_k$ | 0 | … | | |
| | | | ⋮ | ⋮ | ⋮ | | | |
| | | … | 0 | $c_{N-2}$ | 0 | … | | |
| | | … | 0 | $c_{N-1}$ | 0 | … | | |
| | | … | 0 | $c_N$ | 0 | … | | |

Mask in the direction of $270^0$

| | | | | | | | | |
|---|---|---|---|---|---|---|---|---|
| | | | | | | | | |
| | | | | | | | | |
| ⋮ | ⋮ | ⋮ | ⋮ | ⋮ | ⋮ | ⋮ | ⋮ | ⋮ |
| 0 | 0 | 0 | … | 0 | … | 0 | 0 | 0 |
| $c_N$ | $c_{N-1}$ | $c_{N-2}$ | … | $c_k$ | … | $c_2$ | $c_1$ | $c_0$ |
| 0 | 0 | 0 | … | 0 | … | 0 | 0 | 0 |
| ⋮ | ⋮ | ⋮ | ⋮ | ⋮ | ⋮ | ⋮ | ⋮ | ⋮ |
| | | | | | | | | |
| | | | | | | | | |

Mask in the direction of $180^0$

| | | | | | | | | |
|---|---|---|---|---|---|---|---|---|
| | | | | | | | | |
| | | | | | | | | |
| ⋮ | ⋮ | ⋮ | ⋮ | ⋮ | ⋮ | ⋮ | ⋮ | ⋮ |
| 0 | 0 | 0 | … | 0 | … | 0 | 0 | 0 |
| $c_0$ | $c_1$ | $c_2$ | … | $c_k$ | … | $c_{N-2}$ | $c_{N-1}$ | $c_N$ |
| 0 | 0 | 0 | … | 0 | … | 0 | 0 | 0 |
| ⋮ | ⋮ | ⋮ | ⋮ | ⋮ | ⋮ | ⋮ | ⋮ | ⋮ |
| | | | | | | | | |
| | | | | | | | | |

Mask in the direction of $0^0$

| | | | | | | | | |
|---|---|---|---|---|---|---|---|---|
| $c_N$ | 0 | … | | | | | | |
| 0 | $c_{N-1}$ | 0 | … | | | | | |
| ⋮ | 0 | $c_{N-2}$ | 0 | | | | | |
| | ⋮ | 0 | ⋱ | ⋱ | | | | |
| | | ⋮ | 0 | $c_k$ | 0 | ⋮ | | |
| | | | ⋮ | ⋱ | ⋱ | 0 | … | |
| | | | | … | 0 | $c_2$ | 0 | ⋮ |
| | | | | | … | 0 | $c_1$ | 0 |
| | | | | | | … | 0 | $c_0$ |

Mask in the direction of $135^0$

| | | | | | | | | |
|---|---|---|---|---|---|---|---|---|
| | | | | | | … | 0 | $c_0$ |
| | | | | | … | 0 | $c_1$ | 0 |
| | | | | … | 0 | $c_2$ | 0 | ⋮ |
| | | | | ⋱ | ⋱ | 0 | ⋮ | |
| | | … | 0 | $c_k$ | 0 | … | | |
| | ⋮ | 0 | ⋱ | ⋱ | ⋱ | | | |
| ⋮ | 0 | $c_{N-2}$ | 0 | … | | | | |
| 0 | $c_{N-1}$ | 0 | … | | | | | |
| $c_N$ | 0 | … | | | | | | |

Mask in the direction of $225^0$

Figure 8: Different mask

Images a) of the Figures 1, 2 and 3 are the original images while images b), c), d) and f) of Figures 1, 2 and 3 are the results of applying the FDMCF method on the original images with different values of differential order. Images a), b), c), d) and f) of the Figures 4, 5 and 6 are the original image, enhancing result of a) by MPIT, enhancing result of a) by MPITH, enhancing result of a) by HE, enhancing result of a) by FDMC and enhancing result of a) by FDMCF, respectively. On theses figures, we can see that images obtained by the proposed methods look better than those obtained by other methods. For the comparison purpose, we use the contrast of Gray-Level Co-occurrence Matrix (GLCM) in four directions. Tables 1, 2 and 3 are the contrasts of GLCM in four directions. From these tables we can conclude that the proposed methods outperform HE, MPIT and MPITH methods. Based on the results shown in Figures 4, 5 and 6 we can see that the proposed methods are more effectives than the HE, MPIT and MPITH methods, since they enhance better the visual appearance of an image and make it clearer.

# 5 Conclusion

In this paper, we proposed construction of fractional differential masks using Caputo and Caputo-Fabrizio fractional derivatives. Experiments results showed that filtered images by the proposed methods have better visual appearance. Moreover, the proposed techniques have demonstrated a good performance with higher GLCM values.

# References

[1] Ajou, A.; Oqielat, M. N.; Al-Zhour, Z.; Kumar, S. and Momani, S.; *Solitary solutions for time-fractional nonlinear dispersive PDEs in the sense of conformable fractional derivative*, Chaos (2019), **29** (2019), 093102.

[2] Al-Zhour, Z.; Barfeie, M.; Soleymani, F. and Tohidi, E.; *A computational method to price with transaction costs under the nonlinear Black-Scholes model*, Chaos, Solitons & Fractals, **127** (2019), 291–301.

[3] Andrade, A. M. F.; Lima, E. G. and Dartora, C. A.; *An introduction to fractional calculus and its Applications in Electric Circuits*, Revista Brasileira de Ensino de Física, **40** (2018), e3314.

[4] Atangana, A. and Baleanu, D.; *New fractional derivatives with nonlocal and non-singular kernel: Theory and application to heat transfer model*, arXiv preprint, arXiv:1602.03408 (2016).

[5] Baleanu, D.; Diethelm, K.; Escalas, E.; and Trujillo, J. J.; *Fractional Calculus: Models and numerical methods*, Series on Complexity, Nonlinearity and Chaos, **3** (2012).

[6] Baleanu, D.; Jajarmi, A.; Sajjadi, S. S. and Mozyrska, D.; *A new fractional model and optimal control of a tumor-immune surveillance with non-singular derivative operator*, Chaos, **29** (2019), 083127.

[7] Caputo, M. and Fabrizio, M.; *A new Definition of Fractional Derivative without Singular Kernel*, Progr. Fract. Differ. Appl., **1** (2005), 73–85.

[8] Concezzi, M. and Spigler, R.; *Identifying the Fractional Orders in Anomalous Diffusion Models from Real Data*, Fractal Fract., **2**(1) (2014), 14.

[9] El-Ajou, A.; Al-Zhour, Z.; Oqielat, M.; Momani, S. and Hayat, T.; *Series Solutions of Nonlinear Conformable Fractional KdV-Burgers Equation with Some Applications*, The European Physical Journal Plus, **134** (2019), 402.

[10] El-Ajou, A.; Oqielat, M.; Al-Zhour, Z. and Momani, S.; *Analytical Numerical Solutions of the Fractional Multi-Pantograph System: Two Attractive Methods and Comparisons*, Results in Physics, **14** (2019), 102500.

[11] El-Ajou, A.; Oqielat, M.; Al-Zhour, Z.; Kumar, S. and Momani, S.; *Solitary solutions for time-fractional nonlinear dispersive PDEs in the sense of conformable fractional derivative*, Chaos, **29** (2019), 093102.

[12] Garg, P. and Jain, T.; *A comparative study on histogram equalization and cumulative histogram equalization*. International Journal of technology and research, **3**(9) (2017), 41–43.

[13] Goufo, E. F. D. and Mugisha, S. B.; *Similarities in a fifth-order evolution equation with and with no singular kernel*, Chaos, Solitons & Fractals, **130** (2020), 10946.

[14] Jajarmi, A.; Arshad, S. and Baleanu, D.; *A new fractional modelling and control strategy for the outbreak of dengue fever*, Physica A., **535** (2019), 122524.

[15] Jajarmi, A.; Baleanu, D.; Sajjadi, S. S. and Asad, J. H.; *A new feature of the fractional Euler-Lagrange equations for a coupled oscillator using a nonsingular operator approach*, Frontiers in Physics, **7** (2019), 00196.

[16] Jajarmi, A.; Ghanbari, B. and Baleanu, Dumitru. *A new and efficient numerical method for the fractional modelling and optimal control of diabetes and tuberculosis co-existence*, Chaos, **29** (2019), 093111.

[17] Kilbas, A. A.; Srivastava, H. M. and Trujillo, J. J.; *Theory and Applications of Fractional Differential Equations*, North Holland Mathematics Studies, **204** (2006).

[18] Kumar, S.; *A new fractional modeling arising in engineering sciences and its analytical approximate solution*, Alexandria Engineering Journal, **52** (2013), 813–819.

[19] Kumar, S.; Kumar, A.; Abbas, S.; Al Qurashi, M. and Baleanu, D.; *A modified analytical approach with existence and uniqueness for fractional Cauchy reaction-diffusion equations*, Advances in Difference Equations, **2020**(1) (2020), 1–18.

[20] Kumar, S.; Kumar, A. and Nisar, K. S.; *Numerical solutions of nonlinear fractional model arising in the appearance of the strip patterns in two dimensional systems*, Advances in Difference Equations, **413** (2019).

[21] Kumar, R.; Kumar, S.; Singh, J. and Al-Zhour, Z. *A comparative study for fractional chemical kinetics and carbon dioxide $CO_2$ absorbed into phenyl glycidyl ether problems*, Mathematics, **5**(4) (2020), 3201–3222.

[22] Kumar, S.; Nisar, K. S.; Kumar, R.; Cattani, C. and Samet, B.; *A new Rabotnov fractional-exponential function based fractional derivative for diffusion equation under external force*, Mathematical Methods in Applied Science, **43** (2020), 4460–4471.

[23] Liang, X.; Gao, F.; Zhou, C. B.; Wang, Z. and Yang, X. J.; *An anomalous diffusion model based on a new general fractional operator with the Mittag-Leffler function of Wiman type*, Advances in Difference Equations, **18**(1) (2018), 25.

[24] Losada, J. and Nieto, J.; *Properties of a New Fractional Derivative without Singular Kernel*, Progr. Fract. Differ. Appl., **1** (2015), 87–92.

[25] Mboro Nchama, G. A.; Alfonso, L. L.; León Mecías, A. M. and Rodríguez Richard, M.; *Construction of Caputo-Fabrizio fractional differential mask for image enhancement*, Progress in Fractional Differentiation and Application (2020).

[26] Mboro Nchama, G. A.; León Mecías, A. M. and Rodríguez Ricard, M.; *Perona-Malik model with diffusion coefficient depending on fractional gradient via Caputo-Fabrizio derivative*, Abstract and Applied Analysis (2020), **2020** (2020), 15 pages.

[27] Mboro-Nchama, G. A.; Mecías, A. L. and Ricard, M. R.; *The Caputo-Fabrizio fractional integral to generate some new inequalities*, Information Sciences Letters, **8** (2019), 73–80.

[28] Mboro-Nchama, G. A.; Mecías, A. L. and Ricard, M. R.; *Properties of the Caputo-Fabrizio fractional derivative*, Applied Mathematics & Information Sciences, **14** (2020), 1–10.

[29] Mboro Nchama, G. A.; *New fractional integral inequalities via Caputo-Fabrizio operator and an open problem concerning an integral inequality*, New trends in Mathematical Sciences (2020), **8**(2) (2020), 9–21.

[30] Mboro Nchama, G. A.; *On open problems concerning Riemann-Liouville fractional integral inequality*, Mediterranean Journal of Modeling and Simulation, **11** (2019), 001–008.

[31] Mboro-Nchama, G. A.; *Properties of Caputo-Fabrizio fractional operators*, New Trends in Mathematical Sciences, **8** (2020), 1–25.

[32] Morales-Delgado, V. F.; Gómez-Aguilar, J. F. and Taneco-Hernández, M. A.; *Analytical solutions of electrical circuits described by fractional conformable derivatives in Liouville-Caputo sense*, International Journal of Electronics and Communications, **85** (2018), 108–117.

[33] Nandal, A.; Gamboa-Rosales, H.; Dhaka, A.; Celaya-Padilla, J. M.; Galvan-Tejada, J. I.; Galvan-Tejada, C. E.; Martinez-Ruiz, F. J. and Guzman-Valdivia, C.; *Image edge detection using fractional calculus with feature and contrast enhancement.* Circuits, Systems, and Signal Processing, **37**(9) (2018), 3946–3972.

[34] Odham, K. B. and Spanier, J.; *The Fractional Calculus*, Academic Press (1984), New York.

[35] Oqielat, M.; El-Ajou, A.; Al-Zhour, Z.; Alkhasawneh, R. and Alrabaiah, H.; *Series solutions for nonlinear time-fractional Schrdinger equations: Comparisons between conformable and Caputo derivatives*, Alexandria Engineering Journal (2020).

[36] Polubny, I.; *Fractional Differential Equations*, Academic Press (1999), New York.

[37] Pu, Y.; *Application of fractional differential approach to digital image processing.* Journal of Sichuan University, **39**(3) (2007), 124–132.

[38] Pu, Y.; Wang, W.; Zhou, J. et al. *Fractional differential approach to detecting texture features of digital image and its fractional differential filter implementation*, Sci. China Ser. F, Inf. Sci.; **38**(12) (2008), 2252–2272.

[39] Qing-li, C.; H. Guo, H. and Xiu-qiong, Z.; *A Fractional Differential Approach to Low Contrast Image Enhancement*, International Journal of Knowledge and Language Processing (2012), **3**(2) (2012), 20–27.

[40] Ramírez, C.; Astorga, V.; Nuñez, H.; Jaques, A. and Simpson, R.; *Anomalous diffusion based on fractional calculus approach applied to drying analysis of apple slices: The effects of relative humidity and temperature*, Food Process Engineering (2017), **40** (5) (2017), e12549.

[41] Rchid, M.; Ammi, S. and Jamiai, I.; *Finite difference and Legendre spectral method for a time-fractional diffusion-convection equation for image restoration*, Discrete and Continuous Dynamical Systems Series, **11** (2018), 103–117.

[42] Sabatier, J.; Agrawal, O. P. and Machado, J. A. T.; *Advanced in Fractional Calculus: Theoretical Developments and Applications in Physics and Engineering*, Springer (2007).

[43] Sikora, R.; *Fractional derivatives in electrical circuit theory critical remarks*, Archives of Electrical Engineering, **66** (2017), 155–163.

[44] Surya Prasath, V. B.; *Image denoising by anisotropic diffusion with inter-scale information fusion*, Pattern Recognition and Image Analysis, **27** (2017), 748–753.

[45] Yirenkyi, P. A.; Appati, J. K. and Dontwi, I. K.; *A new construction of a fractional derivative mask for image edge analysis based on Riemann-Liouville fractional derivative.* Advances in Difference Equations (2016), DOI 10.1186/s13662-016-0946-8, pp. 1-21.

[46] Yu, J.; Zhai, R.; Zhou, S. and Tan, L.; *Image Denoising Based on Adaptive Fractional Order with Improved PM Model*, Mathematical Problems in Engineering (2018), Article ID 9620754.

[47] Zhang, Y.; Pu, Y. and Zhou, J.; *Construction of Fractional differential Masks Based on Riemann-Liouville Definition.* Journal of Computational Information Systems, **6** (2010), 3191–3198.